

JPMTR-2217  
DOI 10.14622/JPMTR-2217  
UDC 778-186:004.93-021.254

Original scientific paper | 170  
Received: 2022-07-03  
Accepted: 2022-11-18

# Image contrast enhancement by optimization of color channel difference using bat algorithm

Saorabh Kumar Mondal<sup>1</sup>, Arpitam Chatterjee<sup>2</sup> and Bipan Tudu<sup>3</sup>

<sup>1</sup>Department of Applied Electronics and Instrumentation Engineering,  
Haldia Institute of Technology, Haldia, India

arpitam.chatterjee@jadavpuruniversity.in

<sup>2</sup>Department of Printing Engineering, Jadavpur University, Kolkata, India

<sup>3</sup>Department of Instrumentation and Electronics Engineering,  
Jadavpur University, Kolkata, India

## Abstract

Contrast enhancement is a popular image processing technique across different applications. Despite simplicity, many of the reported techniques lack in retention of original image features and cause different artifacts due to over or under enhancement. Such limitations cause problems in cases when the contrast enhancement is used prior to computer vision tasks. This paper presents a new approach of contrast enhancement where the color channel difference has been optimized using bat algorithm to obtain better contrast, improved naturalness and original image feature retention. The potential of the presented method has been assessed with the low contrast images from standard databases and found to be competitive to established models. At the same time the use of device independent color space provides more versatility of the presented method across different applications.

**Keywords:** image processing technique, image enhancement, color difference estimation, color space dynamics

## 1. Introduction

Image contrast is an important characteristic that drives the visual appearance as well as the feature detection tasks for many computer vision applications. Several natural and hardware limitations of the image capturing devices cause low image contrast. Therefore, image contrast enhancement is a prominent research topic. Broadly, the different algorithms for contrast enhancement can be divided into two categories, spatial domain and frequency domain operations. The various techniques under spatial domain have been consolidated in the works of Mustafa and Kader (2018), and Vijayalakshmi, Nath and Acharja (2020). According to Das, Gulati and Mittal (2015), some of the major developments are global histogram equalization (GHE), brightness preserving bi-histogram equalization (BBHE), dualistic sub-image histogram equalization (DSIHE), minimum mean brightness error bi-histogram equalization (MMBEBHE), adaptive histogram equalization (AHE), contrast limited adaptive histogram equalization (CLAHE), adaptive gamma correction (AGC) and adaptive gamma correction weighted distribution (AGCWD); in addition, Sheet, et al. (2010) mention dynamic histo-

gram equalization (DHE) and dynamic fuzzy histogram equalization (DFHE). Some of the later developments in this paradigm includes contrast enhancement using feature preservation bi-histogram equalization (CEFPBHE) (Wang and Chen, 2018), variance-based brightness preserved dynamic histogram equalization for image contrast enhancement (VBBPDHE) (Dhal, et al., 2018), and recursive median and mean partitioned one-to-one grey level mapping transformations for image enhancement (RMMGHT) (Eswar Reddy and Ramachandra Reddy, 2019), two-dimensional histogram equalization (2DHE) (Celik, 2012) and residual spatial entropy based contrast enhancement using discrete cosine transform (RESECEDCT) (Celik and Li, 2016), which provide superior visual contrast. Single scale Retinex (SSR), and multi scale Retinex (MSR) (Zhang, et al., 2017; Petro, Sbert and Morel, 2014) and adaptive MSR (AMSR) models (Lee, Lien and Han, 2014) are some of the Retinex model based developments that have also shown significant improvement over conventional techniques. Contrast-limited adaptive histogram equalization with dual gamma correction (CLAHE-DGC) (Chang, et al., 2018), adaptive gamma correction with weighted histogram distribution (AGCWHDD)

(Veluchamy and Subramani, 2019), fuzzy dissimilarity adaptive histogram equalization with gamma correction (FDAHE-GC) (Veluchamy and Subramani, 2020), and fuzzy dissimilarity histogram (FDH) (Sheet, et al., 2010) are some of the techniques that employ gamma correction. Frequency domain algorithms have shown better performance over spatial domain approaches in many cases since transform domains provide better control over local image characteristics, which in turn provides improved feature retention. Discrete cosine transform (DCT) coefficient scaling (DCTCS) (Samani, Panetta and Agaian, 2016), DCT coefficient histogram (DCTCH) (Panetta, Xia and Agaian, 2012), and DCT pyramid and singular value decomposition (DCT-SVD) (Atta and Ghanbari., 2013) are some of the noted works in this paradigm. Spatial entropy-based contrast enhancement in DCT (SECEDCT) (Celik, 2014) is one of the recent image enhancement techniques, which is the modification of SECE technique in DCT domain. The survey reveals that the scope of improvement is still open, especially, in terms of higher degree of naturalness and image feature retention in enhanced images, which are commonly lacking due to either over- or under-enhancements. At the same time, many of these algorithms provide compromised results in case the contrast distortion is in higher extent.

The applications of different soft computing techniques have as well been reported for image enhancement. Swarm intelligence techniques are one of the subsets of soft computing techniques where the algorithms mimic the behaviors of natural swarms. Particle swarm optimization (PSO), artificial bee colony optimization (ABC), and ant colony optimization (ACO) (Gad, 2022) are popular algorithms that have been employed for contrast enhancement. The elimination of pixel groups based on their contribution towards image detailing has been performed by mean-shift algorithm and then moth swarm algorithm has been employed to maximize the Kullback–Leibler entropy towards contrast enhancement (Luque-Chang, et al., 2021). A novel krill herd based optimization has also been applied in plateau limited histogram clipping for contrast enhancement of medical images (Kandhway, Bhandari and Singh, 2020). To improve the contrast of industrial images a novel ant lion optimization algorithm has been applied and found competitive results over other metaheuristics of swarm intelligence (Yue and Zhang, 2021). Bat algorithm (BA) was developed mimicking the food searching behavior of bat. It has shown promising potential in diverse applications (Asokan, et al., 2020) including feature preserving contrast enhancement.

This paper presents a more general and versatile approach for contrast enhancement. The contribution of the paper is two-fold; a new color channel difference based estimation of lightness that influences the

image contrast to a great extent and application of BA to minimize the statistical moment of the stated lightness estimation. The lightness estimation is motivated by the dark channel priory (DCP) (Tsai, Lin and Guo, 2019) concept but it is computationally less expensive. The motivation of difference channel estimation (DCE) was towards better representation of the lightness distribution in the low contrast images.

## 2. Presented method

### 2.1 Difference channel estimation

There are many obstructions through which reflected light passes before it is captured by camera lenses. Hence, it is a very difficult task to assess the lightness distortion exactly. At the same point in time based on the transmission media (air or water), there are some frequencies of light that can travel more while some cannot because of their wavelength. Color channel can be a possible indicator for the deficiencies in the lightness distribution, which in-turn causes image quality degradation in many aspects including contrast. To address this, difference color channel was estimated. It can be noted here that all color space conversions used in this work were realized through standard conversion formulae (Nishad and Chezian, 2013).

The native color space of the color images is RGB, which was converted to YCbCr using standard conversion formulae for better interpretation of perceived color. In YCbCr color space  $Cr$  and  $Cb$  channels provide the chrominance distribution in blue and red spectrum, respectively. It can be assessed that the difference between  $Cr$  and  $Cb$  is indicative to the light receiving characteristics. For instance, in air blue light travels less distance; hence, the foggy images will have higher energy content in  $Cr$  than in  $Cb$  while in case of underwater image the energy content of  $Cb$  will be higher. To measure the energy difference between  $Cr$  and  $Cb$  both the channel information were converted to the frequency domain using DCT (Xu, Wang and Lu, 2011). The selection of DCT over Fourier transform is motivated by its simplicity and absence of imaginary component.

The distance between the object and the camera lens also contributes towards distortion. For instance, the light needs to travel more if the object is far, which will subject the waveforms to a higher degree of natural distortions. The luminance representation in Y channel of YCbCr can be a possible interpretation of this distance aspect. The closer objects can appear brighter than the far objects. Considering these two factors the difference channel ( $D$ ) was calculated by Equation [1].

$$D = \bar{Y} - \text{abs}(\overline{Cb} - \overline{Cr}) \quad [1]$$

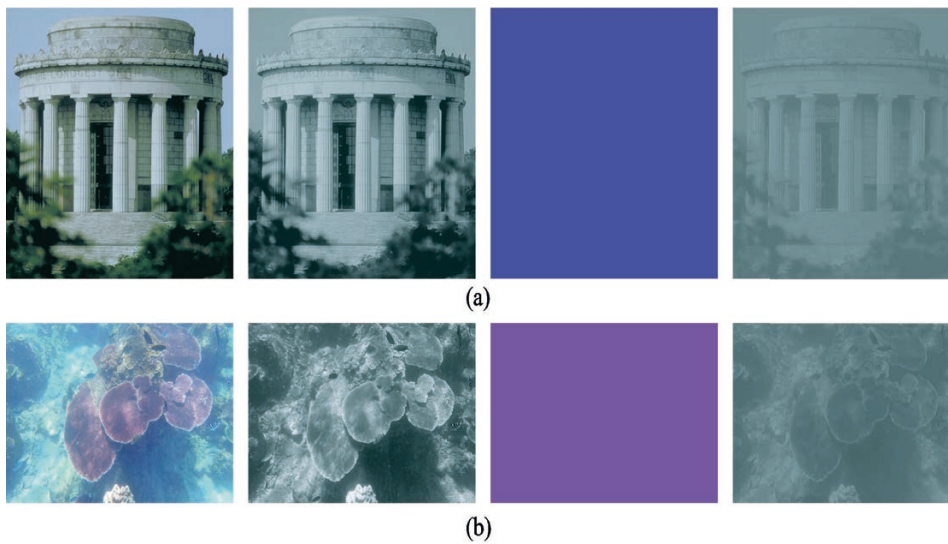


Figure 1: (From left to right) the input images, corresponding difference channel, background light estimation and transmittance for (a) atmospheric and (b) underwater image

where calculation of YCbCr has been done using standard conversion formulae (Fashandi, Peters and Ramanna, 2009) and  $\overline{Y}$ ,  $\overline{Cb}$ ,  $\overline{Cr}$  are the DCT of  $Y$ ,  $Cb$ ,  $Cr$  channels, respectively. Further,  $d$  is the spatial domain representation of difference channel transform  $D$ .

The transmittance ( $T$ ) was then estimated using this difference channel transform on the background light weighted input as shown in Equation [2]. The  $Bg$  in Equation [2] corresponds to the background light estimation where  $k$ -means clustering (Oyelade, Oladipupo and Obagbuwa, 2010) has been used in this work. The centroid of 10 % highest values in  $d$  was considered for  $Bg$ . Figure 1 shows examples of the difference channel and transmittance assessment that resulted from the presented method;  $\eta$  is the assumed effective wide-band attenuation coefficient (Akkaynak, et al., 2017), which depends on the light scattering media (surface/underwater) under consideration.

$$T = 1 - \eta d(M) \quad [2]$$

where

$$M = (I/Bg)_{c \in \text{YCbCr}}$$

## 2.2 Optimization using bat algorithm

The transmittance was subjected to optimization using BA. The BA has some major advantages over other popular metaheuristics in terms of simplicity, lesser parameter tuning requirements and robustness (Wang and Li, 2019). It initiates optimization with random solutions generated in the problem space. This generation can be guided towards faster convergence. The algorithm is driven using the echolocation charac-

teristics of bats that they use to search for food. Each bat updates their position and velocity at every iteration based on their best position and velocity information at each iteration. As the bat approaches closer to the prey the loudness of the emitted sound decreases while the pulse emission rate increases. The BA algorithm can be presented as pseudo code presented in Appendix.

### 2.2.1 Objective function formulation

To achieve the well distributed histogram in transmittance image it was converted to device independent HSV color space from its YCbCr color space using standard conversion formulae. The  $V$  channel was extracted from the resulting HSV image, which was further subjected to calculation of the L2 norm of the input and enhanced image feature vector as shown in Equation [3], where  $dh$  and  $eh$  represent the DCT of  $V$  channel histogram information. The feature vector in this work is the DCT of  $V$  channel histogram. This L2 norm based similarity measurement can address the feature similarity (Fashandi, Peters and Ramanna, 2009) and has been used as one of the parameters ( $\varphi_1$ ) in the objective function  $\varphi$ .

$$\varphi_1 = \left( \sum_{i=1}^n (dh_i - eh_i)^2 \right)^{1/2} \quad [3]$$

The second parameter of the objective function has been developed based on the skewness and kurtosis of  $dh$  and  $eh$ . The plot of original  $V$  channel histogram is negatively or positively skewed (as it can be seen in Figure 3 in the Results section). The target was to reduce the skewness towards zero and maintain the kurtosis near the value of 3 considering the standard

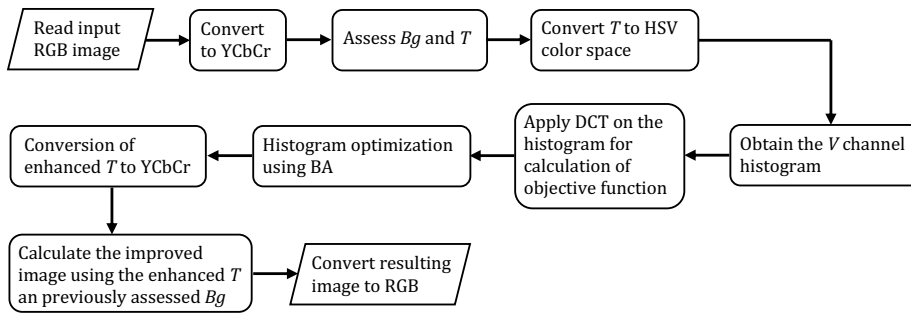


Figure 2: Overview of the proposed contrast enhancement method

normal distribution (Kallner, 2018). Therefore, the second parameter of  $\varphi$  ( $\varphi_2$ ) has been formulated as expressed in Equation [4].

$$\varphi_2 = \text{skewness}(eh) + (3 - \text{kurtosis}(eh)) \quad [4]$$

Combining the above two parameters the objective function has been formulated as Equation [5]. In the presented work both parameters have been equally weighted ( $w_1 = w_2 = 0.5$ ). However, depending on the applications or modeling requirements they can be modulated maintaining their sum to unity, i.e.,  $w_1 + w_2 = 1$ .

$$\varphi = w_1\varphi_1 + w_2\varphi_2 \quad [5]$$

Apart from contrast the low quality images lack colorfulness as well. Though the primary goal of this work is towards contrast enhancement, a simple gamma scaling of the saturation channel has also been included to address the colorfulness issue. A global gamma based scaling can cause unnaturalness in enhanced image, which may result in over-enhancement. To avoid that the DCE has been used to assess the pixels to which the scaling has been applied. The pixels with insufficient color information have been identified by a thresholding operation. The thresholding operation generates a mask, which has been used upon the  $S$  channel and further subjected to a gamma scaling as shown in Equation [6].

$$\hat{S} = (S \times \hat{d})^\gamma \quad [6]$$

where  $\hat{S}$  is the gamma scaled  $S$  channel,  $\gamma$  is the scaling value and  $\hat{d}$  is the thresholded difference channel mask. The value of  $\gamma$  varies depending on the image information and in this work  $\gamma = -\log_2(\sigma)$  (Rahman, et al., 2016) has been used to calculate  $\gamma$  value of individual image, where  $\sigma$  is the standard deviation of  $S$ .

The enhanced transmittance in HSV domain was then reverted back to YCbCr color space and has been used to assess the distortion free image using the estimated  $Bg$ ,  $T$  and a constant  $1 \times 3$  vector  $t_0$  as shown

in Equation [7] (Hou, et al., 2020) where  $J$  is the contrast enhanced image in YCbCr color space. It can be noted here that values of  $t_0$  in this work were set as [0.8 0.8 0.5] and it was arrived by trial and error with about 200 image samples from different image databases. Finally, the image was converted back to its native RGB format using standard conversion formulae. The proposed method is consolidated as a flowchart in Figure 2.

$$J = \left( Bg - \left( I - \left( Bg - \max_{c \in YCbCr}(T, t_0) \right) \right) \right) \quad [7]$$

In this work the initial population of 10 bats (initial solutions) found to be optimal through trial and error with different number of bats. The length of the solution was 256 since the DCT domain histogram was the initial position of individual bat. The initialization of individual bat position was random but generated within the range of frequencies present in the image under consideration. The values of initial pulse frequencies  $f_{\min}$  and  $f_{\max}$  were set as 0 and 1, respectively. The values for both the constants  $\alpha$  and  $\beta$  were set as 0.92. The maximum number of iterations was set as 100. Similarly, the loudness parameter  $A$  was initiated randomly with  $A_{\min}$  and  $A_{\max}$  and values as 0 and 1, respectively, where resulting  $A_{\min}$  interprets the bat has reached the prey and not emitting any sound. The presented method has been realized using Matlab® in Windows® platform.

### 2.3 Image quality evaluation

Objective evaluations were performed against five popular image quality assessment metrics; image entropy (Wang and Ye, 2005), patch-based contrast quality index (PCQI) (Wang, et al., 2015), natural image quality evaluator (NIQE) (Mittal, Soundararajan and Bovik, 2013), contrast enhancement factor (CEF) and colorfulness (Veluchamy and Subramani, 2020). The choice of these metrics among many others was towards covering different aspects of the image quality. For instance, entropy provides measure of information fidelity while PCQI is towards contrast distortion. Similarly, NIQE is

a blind technique where no reference image is presented to the evaluation. In combination, these metrics can provide information about an overall quality of the image. During evaluation the performance is judged by their values, in particular, for entropy, PCQL, CEF and colorfulness higher values indicate better results while for NIQE lower values indicate better results.

### 3. Results

The test of performance has been performed with images from standard databases (Ponomarenko, et al., 2009; Larson and Chandler, 2010; SIPI, n.d.). Figure 3 shows the histogram of the transmittance estimations

of the input images, narrowness and biased nature to either side of the histogram. After the optimization the histograms of the resulting transmittance estimation are visibly well distributed in the available tonal levels, which undoubtedly improves the contrast as shown in Figure 3.

Figure 4 shows a test image and resulting contrast enhanced output along with the original and enhanced V channel with their corresponding histograms in spatial domain. It can be seen that the image contrast has been visibly improved. The improvement is further evident from the V channel presentation where each element of the image is clearly visible due to improvement in contrast. For instance, the number ‘21’ that is

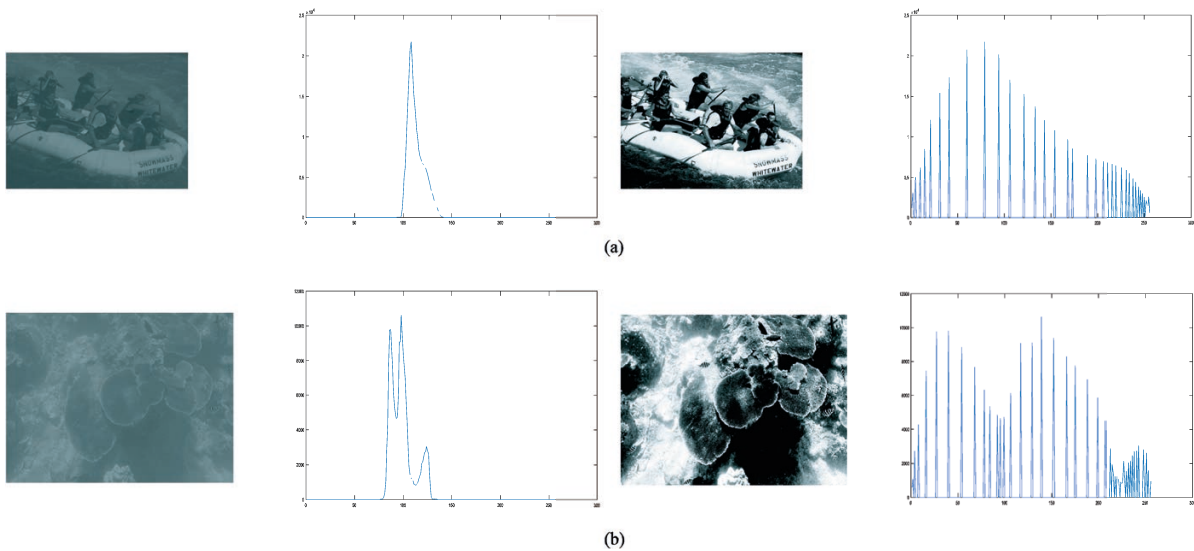


Figure 3: (Left to right) the original transmittance estimation, with corresponding histogram and enhanced transmittance with corresponding histogram for (a) atmospheric and (b) underwater images

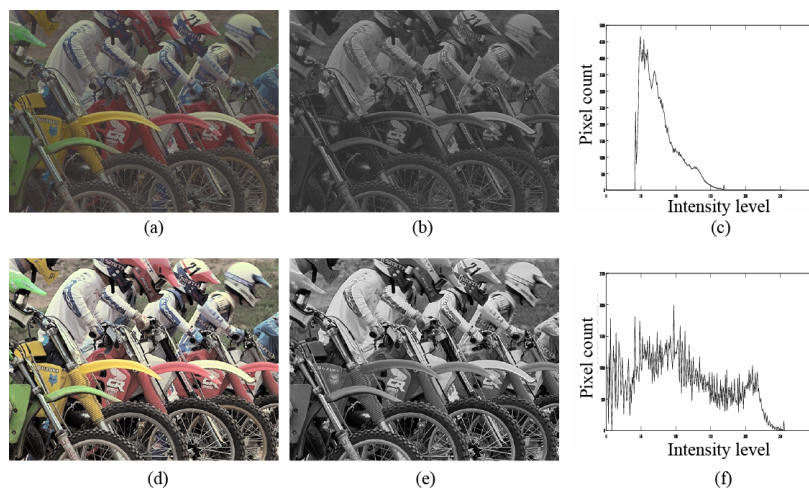


Figure 4: Result of proposed technique with ‘motorcycle’ image; (a) input low contrast image, (b) V channel of input image, (c) histogram of (b), (d) enhanced image, (e) V channel of enhanced image and (f) histogram of (e)

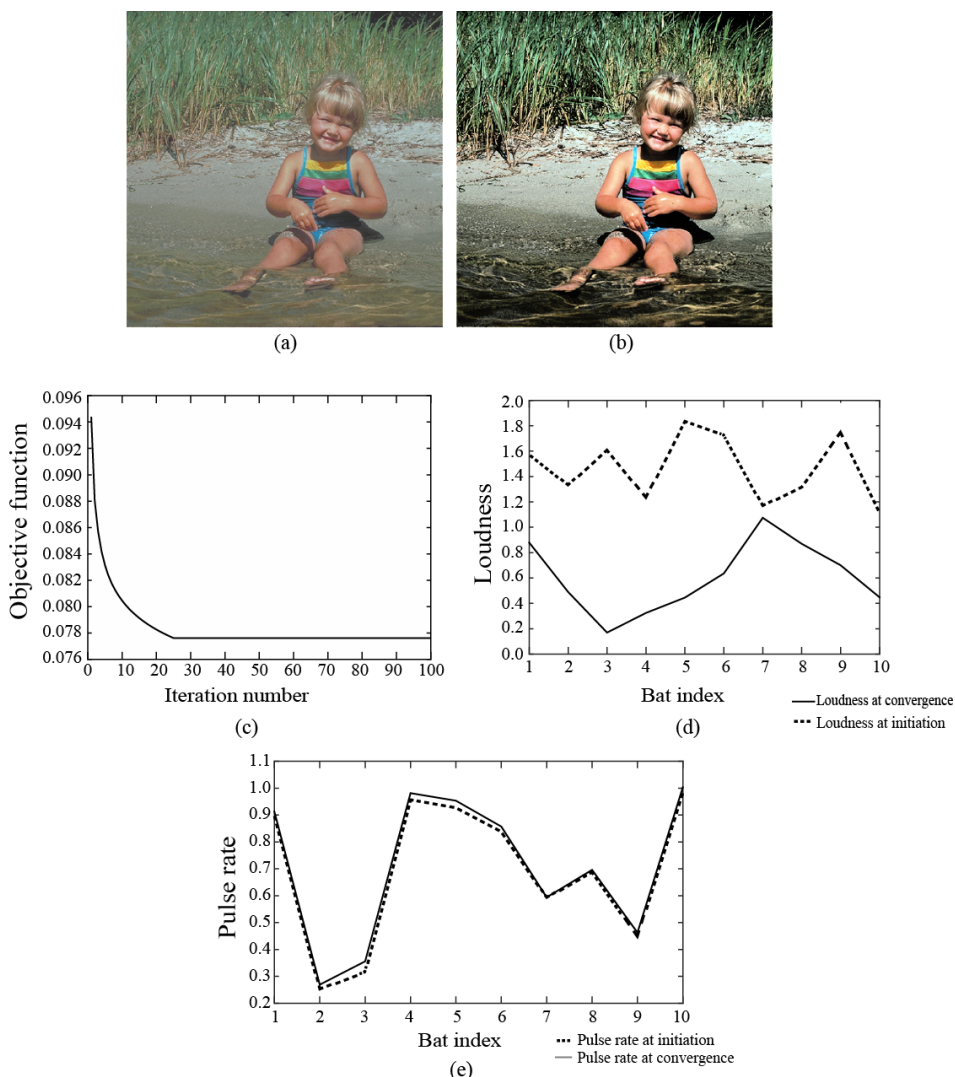


Figure 5: Result of presented method with ‘child’ image and BA dynamics; (a) input low contrast image, (b) enhanced image, (c) convergence curve, (d) loudness reduction and (e) pulse rate increment for each bat at the start and end of the BA

appearing on one of the helmets is not clearly visible in the input image as it is getting mixed with the background. But, as the contrast increases it becomes clearly visible in enhanced image. Such improvements can be crucial in case contrast enhancement is employed prior computer vision tasks for text or object identification. In the respective histogram plot it can also be observed that the enhancement causes substantial expansion of the histogram, which in turn provides better utilization of the entire intensity range instead of a narrow range like in original image.

In Figure 5 the BA dynamics have been presented, that are important for observing the performance of the algorithm and nature of convergence. Figure 5 clearly shows that the algorithm optimizes quickly and comes to a stable state. Also, the reduction of loudness and

increase in pulse rate confirms the desired movement of BA. It also shows that the reported parameter setting can work well for the problem under consideration.

Figure 6 shows the results of proposed method with different contrast distortion levels with test images from CSIQ database. It can be seen that the performance of the proposed method is consistent across different distortion levels.

The colorfulness in the enhancement achieved with the presented method also confirms the naturalness. For instance, the results shown in Figure 6b show the sun ray feature prominently while not introducing excessive whiteness. The preservation of image features is also evident from results of Figure 6c where sharpness and edge retention is clearly visible.

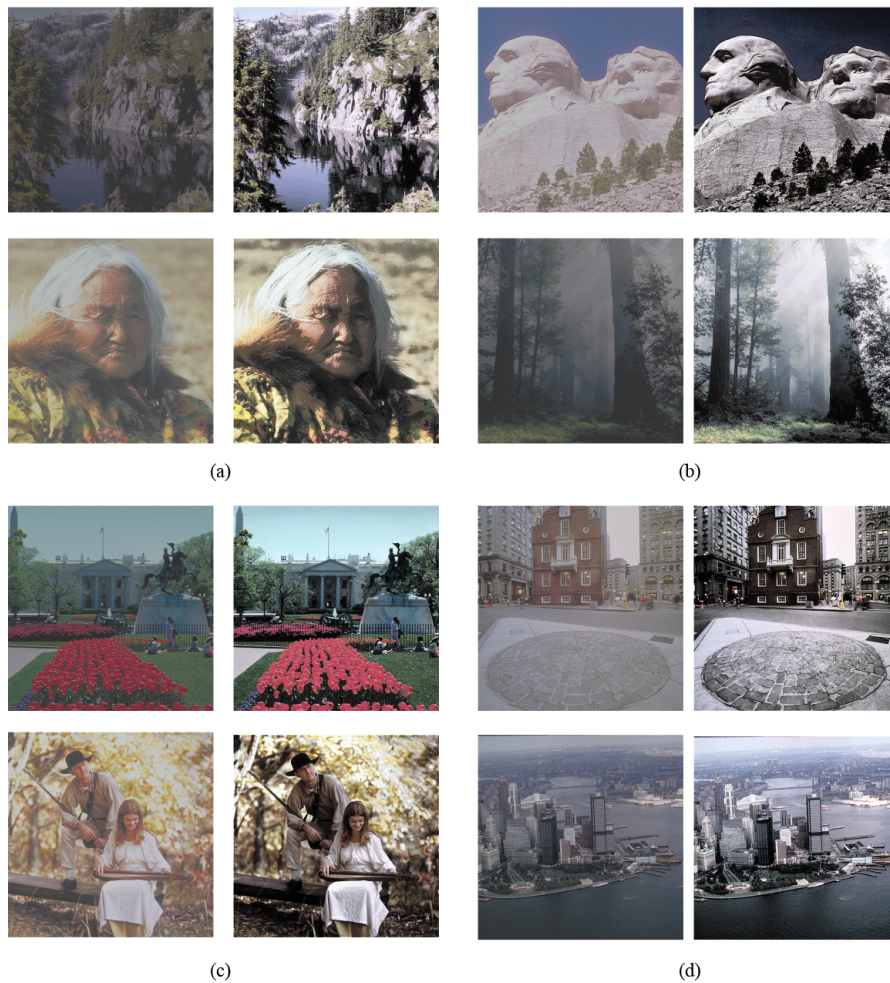


Figure 6: Visual comparison of four pairs of test images at different levels of contrast

#### 4. Discussions

In Figure 7a detailed retention analysis has been presented. It can be seen that in the image enhanced by presented technique the original image details are well retained. Also, the enlarged areas shown in Figures 7b and 7d portray that the presented method can avoid any visual artifacts due to over- or under-enhancement. The method can also provide good lightness distribution while retaining the white color.

To assess the suitability of the presented method across different types of applications, example of results obtained for low contrast underwater image has been shown in Figure 8. It can be seen that most of the techniques under consideration fail to enhance the image quality and suffer from black patches (GHE and CLAHE-DGC), over color effect and failing to produce a natural effect (MSR), degradation of sharpness (SECEDCT), etc. The AGCWHD, FDAHE-GC and proposed technique perform well for maintain the color

and enhance the contrast. But among all techniques mentioned here, the proposed methodology performs much better in terms of contrast enhancement, preserving the brightness, balanced sharpness, and retention of image information.

The mean and standard deviation values for different metrics for 1000 images under consideration have been consolidated in Table 1. In this table the performance of the proposed method has been highlighted in bold font. It clearly shows competitive potential of the presented method against all the metrics under consideration. This also vouches the generosity of the presented method as other techniques have performed well against either of the metrics but not for all the metrics. However, room of improvement in terms of standard deviation values is open in the proposed method.

The PCQI maps shown in Figure 9 are binary images where black patches show the areas of contrast distortions. In this figure SECEDCT shows lots of black

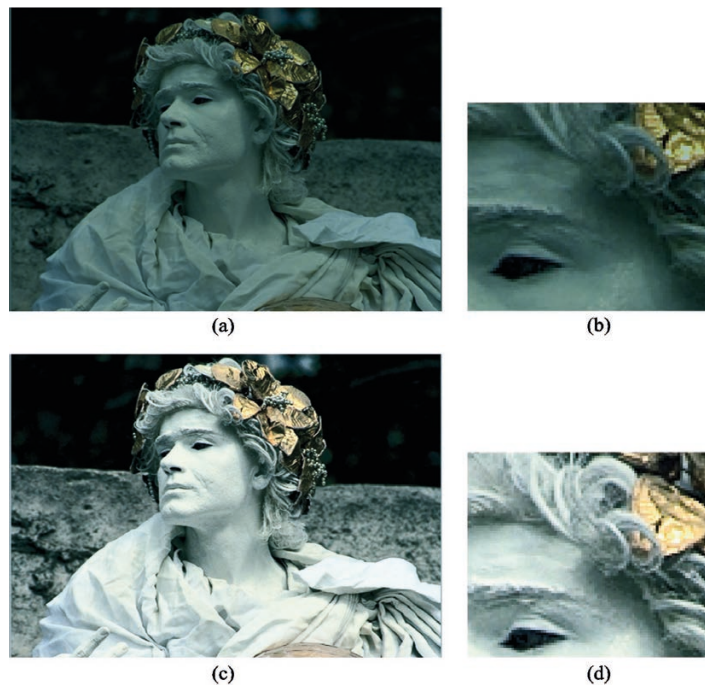


Figure 7: Local improvement analysis with 'statue' image; (a) original low contrast image, (b) the region to focus, (c) enhanced image and (d) the corresponding region shown in (b)

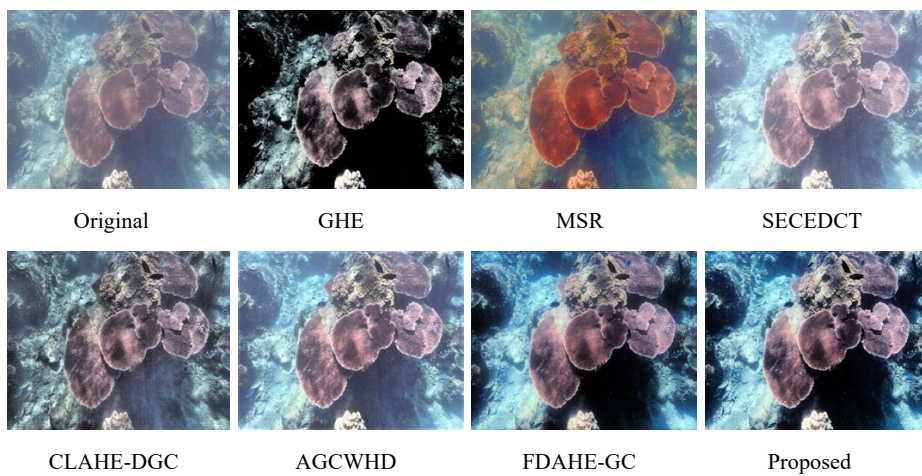


Figure 8: Results of different algorithms with 'underwater' image

Table 1: Objective evaluation of results using the proposed BA method ( $\mu$  stands for mean value, and  $\sigma$  for standard deviation)

Methods	GHE		MSR		SECDCT		CLAHE-DGC		AGCWHD		FDAHE-GC		Proposed	
	$\mu$	$\sigma$	$\mu$	$\sigma$	$\mu$	$\sigma$	$\mu$	$\sigma$	$\mu$	$\sigma$	$\mu$	$\sigma$	$\mu$	$\sigma$
Entropy	7.36	0.66	7.48	0.68	7.34	0.62	7.42	0.52	7.53	0.62	7.62	0.82	<b>7.61</b>	<b>0.60</b>
PCQI	1.11	0.10	1.02	0.09	1.06	0.10	1.16	0.10	1.15	0.08	1.07	0.10	<b>1.18</b>	<b>0.12</b>
NIQE	3.64	1.41	3.51	1.14	3.55	1.60	3.65	1.24	3.58	1.20	3.63	1.33	<b>3.53</b>	<b>1.01</b>
CEF	1.15	0.08	0.98	0.06	0.82	0.05	0.96	0.06	0.86	0.05	1.06	0.06	<b>1.25</b>	<b>0.06</b>
Colorfulness	11.30	1.11	20.72	1.20	13.90	1.02	12.24	1.09	14.68	1.05	17.81	1.07	<b>21.40</b>	<b>1.10</b>

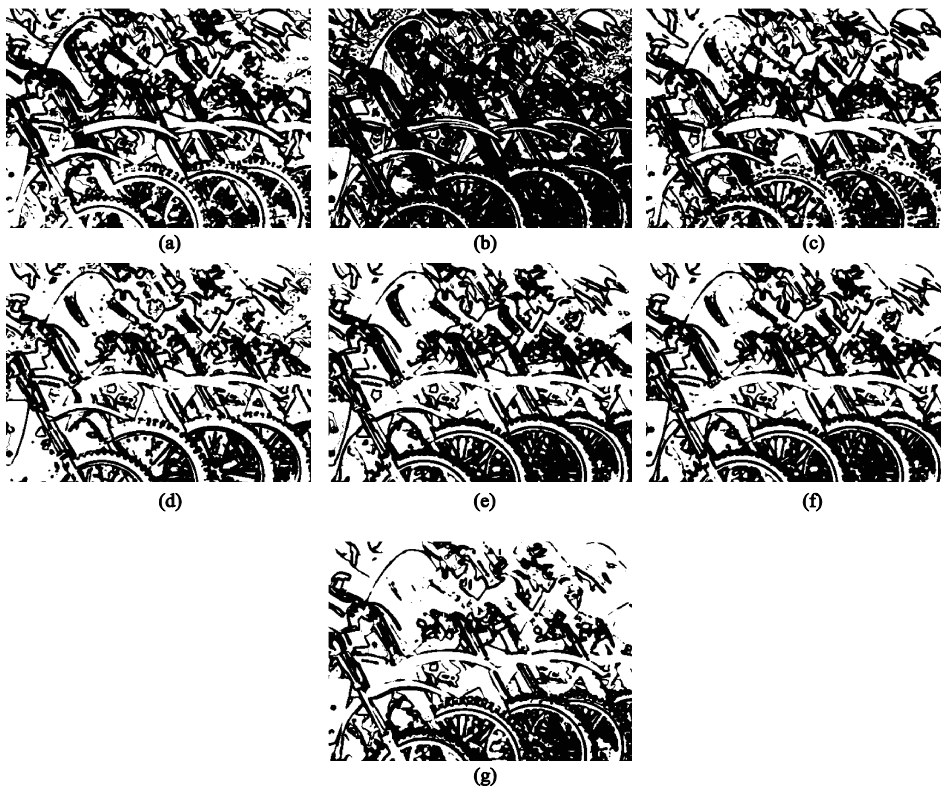


Figure 9: PCQI map (black pixels indicate  $PCQI < 1$ ); (a) MSR, (b) SECEDCT, (c) FDAHE-GC, (d) AGCWHD, (e) GHE, (f) CLAHE-DGC, and (g) proposed BA method

patches representing  $PCQI < 1$  and contrast distortion causing artificial appearance in the resulting image. Similarly, AGCWHD shows a considerably lower amount of black patches causing better output in terms of resulting contrast distortions. Proposed technique provides much lower distortions in most of the areas, which causes a higher mean-PCQI value. The MSR and FDAHE-GC show almost similar amount of distortion, whereas CLAHE-DGC and GHE perform little bit better in the tires of the motorcycles.

## 5. Conclusion

A new concept called DCE has been presented in the paper towards estimation of transmittance assessment. The transmittance enhancement has been pro-

posed in HSV color space and optimization of DCT of the histogram using BA. The fast convergence of the BA provides acceptable processing time and the model based dynamics imparts higher possibility of generalization across different imaging media with the presented model.

The work can be further extended to application in contrast enhancement of medical images where the imaging model is different from the reported ones. The possibilities of improvement can be explored with other bio-inspired optimization algorithms, a more robust fitness or objective function and inclusion of multiple objective paradigms. Considering the possible future scopes the competitive results of the presented method vouch for its potential as a possible addition to the existing standard contrast enhancement method.

### Data availability statement

Used images from databases freely available in public domain.

### Conflict of interest statement

There is no conflict of interest identified for this article.

## References

- Akkaynak, D., Treibitz, T., Shlesinger, T., Loya, Y., Tamir, R. and Iluz, D., 2017. What is the space of attenuation coefficients in underwater computer vision? In: *2017 IEEE Conference on Computer Vision and Pattern Recognition (CVPR)*. Honolulu, HI, USA, 21–26 July 2017, pp. 568–577. <https://doi.org/10.1109/CVPR.2017.68>.
- Asokan, A., Popescu, D.E., Anitha, J. and Hemanth, D.J., 2020. Bat algorithm based non-linear contrast stretching for satellite image enhancement. *Geosciences*, 10(2): 78. <https://doi.org/10.3390/geosciences10020078>.
- Atta, R. and Ghanbari, M., 2013. Low-contrast satellite images enhancement using discrete cosine transform pyramid and singular value decomposition. *IET Image Processing*, 7(5), pp. 472–483. <https://doi.org/10.1049/iet-ipr.2013.0083>.
- Celik, T., 2012. Two-dimensional histogram equalization and contrast enhancement. *Pattern Recognition*, 45(10), pp. 3810–3824. <https://doi.org/10.1016/j.patcog.2012.03.019>.
- Celik, T., 2014. Spatial entropy-based global and local image contrast enhancement. *IEEE transactions on image processing*, 23(12), pp. 5298–5308. <https://doi.org/10.1109/TIP.2014.2364537>.
- Celik, T. and Li, H.-C., 2016. Residual spatial entropy-based image contrast enhancement and gradient-based relative contrast measurement. *Journal of Modern Optics*, 63(16), pp. 1600–1617. <https://doi.org/10.1080/09500340.2016.1163427>.
- Chang, Y., Jung, C., Ke, P., Song, H. and Hwang, J., 2018. Automatic contrast-limited adaptive histogram equalization with dual gamma correction. *IEEE Access*, 6, pp. 11782–11792. <https://doi.org/10.1109/ACCESS.2018.2797872>.
- Das, S., Gulati, T. and Mittal, V., 2015. Image contrast enhancement using AGCWD with region based enhancement. *International Journal of Applied Engineering Research*, 10(11), pp. 30109–30119.
- Dhal, K.G., Das, A., Ghoshal, N. and Das, S., 2018. Variance based brightness preserved dynamic histogram equalization for image contrast enhancement. *Pattern Recognition and Image Analysis*, 28(4), pp. 747–757. <https://doi.org/10.1134/S1054661818040211>.
- Eswar Reddy, M. and Ramachandra Reddy, G., 2019. Recursive median and mean partitioned one-to-one gray level mapping transformations for image enhancement. *Circuits, Systems, and Signal Processing*, 38(7), pp. 3227–3250. <https://doi.org/10.1007/s00034-018-1013-3>.
- Fashandi, H., Peters, J. and Ramanna, S., 2009. L2 norm length-based image similarity measures: concrescence of image feature histogram distances. In: *Proceedings of the 11<sup>th</sup> IASTED International Conference on Signal and Image Processing (SIP 2009)*. Honolulu, HI, USA, 17–19 August 2009. ACTA Press, pp. 178–185.
- Gad, A.G., 2022. Particle swarm optimization algorithm and its applications: a systematic review. *Archives of Computational Methods in Engineering*, 29(5), pp. 2531–2561. <https://doi.org/10.1007/s11831-021-09694-4>.
- Hou, G., Zhao, X., Pan, Z., Yang, H., Tan, L. and Li, J., 2020. Benchmarking underwater image enhancement and restoration, and beyond. *IEEE Access*, 8, pp. 122078–122091. <https://doi.org/10.1109/ACCESS.2020.3006359>.
- Kallner, A., 2018. *Laboratory statistics: methods in chemistry and health sciences*. 2<sup>nd</sup> ed. Amsterdam, Oxford, Cambridge: Elsevier. <https://doi.org/10.1016/B978-0-12-814348-3.00001-0>.
- Kandhway, P., Bhandari, A.K. and Singh, A., 2020. A novel reformed histogram equalization based medical image contrast enhancement using krill herd optimization. *Biomedical Signal Processing and Control*, 56: 101677. <https://doi.org/10.1016/j.bspc.2019.101677>.
- Larson, E.C. and Chandler, D.M., 2010. Most apparent distortion: full-reference image quality assessment and the role of strategy. *Journal of Electronic Imaging*, 19(1): 011006. <https://doi.org/10.1117/1.3267105>.
- Lee, C.-H., Lien, C.-C. and Han, C.-C., 2014. Color image enhancement using multiscale Retinex and image fusion techniques. *World Academy of Science, Engineering and Technology International Journal of Computer and Information Engineering*, 8(10), pp. 1796–1802. <https://doi.org/10.5281/zenodo.1096355>.
- Luque-Chang, A., Cuevas, E., Pérez-Cisneros, M., Fausto, F., Valdivia-González, A. and Sarkar, R., 2021. Moth swarm algorithm for image contrast enhancement. *Knowledge-Based Systems*, 212: 106607. <https://doi.org/10.1016/j.knosys.2020.106607>.
- Mittal, A., Soundararajan, R. and Bovik, A.C., 2013. Making a “completely blind” image quality analyzer. *IEEE Signal Processing Letters*, 20(3). pp. 209–212. <https://doi.org/10.1109/LSP.2012.2227726>.
- Mustafa, W.A. and Kader, M.M.M.A., 2018. A review of histogram equalization techniques in image enhancement application. *Journal of Physics: Conference Series*, 1019: 012026. <https://doi.org/10.1088/1742-6596/1019/1/012026>.
- Nishad, P.M. and Chezian, R.M., 2013. Various colour spaces and colour space conversion algorithms. *Journal of Global Research in Computer Science*, 4(1), pp. 44–48.
- Oyelade, O.J., Oladipupo, O.O. and Obagbuwa, I.C., 2010. Application of k-means clustering algorithm for prediction of students’ academic performance. *International Journal of Computer Science and Information Security*, 7(1), pp. 292–295 (arXiv:1002.2425 abs/1002.2425). <https://doi.org/10.48550/arXiv.1002.2425>.
- Panetta, K.A., Xia, J. and Agaian, S.S., 2012. Color image enhancement based on the discrete cosine transform coefficient histogram. *Journal of Electronic Imaging*, 21(2): 021117. <https://doi.org/10.1117/1.JEI.21.2.021117>.
- Petro, A.B., Sbert, C. and Morel, J.-M., 2014. Multiscale Retinex. *Image Processing On Line*, 4, pp. 71–88. <https://doi.org/10.5201/ipol.2014.107>.

- Ponomarenko, N., Lukin, V., Zelensky, A., Egiazarian, K., Astola, J., Carli, M. and Battisti, F., 2009. TID2008 – a database for evaluation of full-reference visual quality assessment metrics. *Advances of Modern Radioelectronics*, 10(4), pp. 30–45.
- Rahman, S., Rahman, M.M., Abdullah-Al-Wadud, M., Al-Quaderi, G.D. and Shoyaib, M., 2016. An adaptive gamma correction for image enhancement. *EURASIP Journal on Image and Video Processing*, 35. <https://doi.org/10.1186/s13640-016-0138-1>.
- Samani, A., Panetta, K. and Agaian, S., 2016. Contrast enhancement for color images using discrete cosine transform coefficient scaling. In: *2016 IEEE Symposium on Technologies for Homeland Security (HST)*. Waltham, MA, USA, 10–11 May 2016. IEEE. <https://doi.org/10.1109/THS.2016.7568968>.
- Sheet, D., Garud, H., Suveer, A., Mahadevappa, M. and Chatterjee, J., 2010. Brightness preserving dynamic fuzzy histogram equalization. *IEEE Transactions on Consumer Electronics*, 56(4), pp. 2475–2480. <https://doi.org/10.1109/TCE.2010.5681130>.
- SIPI, n.d. The USC-SIPI image database. [online] Available at: <<http://sipi.usc.edu/database/>> [Accessed March 2021].
- Tsai, C.-C., Lin, C.-Y. and Guo, J.-I., 2019. Dark channel prior based video dehazing algorithm with sky preservation and its embedded system realization for ADAS applications. *Optics Express*, 27(9), pp. 11877–11901. <https://doi.org/10.1364/OE.27.011877>.
- Veluchamy, M. and Subramani, B., 2019. Image contrast and color enhancement using adaptive gamma correction and histogram equalization. *Optik*, 183, pp. 329–337. <https://doi.org/10.1016/j.ijleo.2019.02.054>.
- Veluchamy, M. and Subramani, B., 2020. Fuzzy dissimilarity color histogram equalization for contrast enhancement and color correction. *Applied Soft Computing*, 89: 106077. <https://doi.org/10.1016/j.asoc.2020.106077>.
- Vijayalakshmi, D., Nath, K.N. and Acharja, O.P., 2020. A comprehensive survey on image contrast enhancement techniques in spatial domain. *Sensing and Imaging*, 21(1): 40. <https://doi.org/10.1007/s11220-020-00305-3>.
- Wang, X. and Chen, L., 2018. Contrast enhancement using feature-preserving bi-histogram equalization. *Signal, Image and Video Processing*, 12(4), pp. 685–692. <https://doi.org/10.1007/s11760-017-1208-2>.
- Wang, J.-S. and Li, S.-X., 2019. An improved grey wolf optimizer based on differential evolution and elimination mechanism. *Scientific Reports*, 9: 7181. <https://doi.org/10.1038/s41598-019-43546-3>.
- Wang, S., Ma, K., Yeganeh, H., Wang, Z. and Lin, W., 2015. A patch-structure representation method for quality assessment of contrast changed images. *IEEE Signal Processing Letters*, 22(12), pp. 2387–2390. <https://doi.org/10.1109/LSP.2015.2487369>.
- Wang, C. and Ye, Z., 2005. Brightness preserving histogram equalization with maximum entropy: a variational perspective. *IEEE Transactions on Consumer Electronics*, 51(4), pp. 1326–1334. <https://doi.org/10.1109/TCE.2005.1561863>.
- Xu, Z.J., Wang, Z.Z. and Lu, Q., 2011. Research on image watermarking algorithm based on DCT. *Procedia Environmental Sciences*, 10, Part B, pp. 1129–1135. <https://doi.org/10.1016/j.proenv.2011.09.180>.
- Yue, X. and Zhang, H., 2021. A novel industrial image contrast enhancement technique based on an improved ant lion optimizer. *Arabian Journal for Science and Engineering*, 46(4), pp. 3235–3246. <https://doi.org/10.1007/s13369-020-05148-4>.
- Zhang, S., Wang, T., Dong, J. and Yu, H., 2017. Underwater image enhancement via extended multi-scale Retinex. *Neurocomputing*, 245, pp. 1–9. <https://doi.org/10.1016/j.neucom.2017.03.029>.

### Appendix: Pseudo code of BA

Initial population of bat  $X (x_1, x_2, \dots, x_n)$  and associated initial velocity of each bat  $(v_1, v_2, \dots, v_n)$

Generation

Fitness calculation of each bat using the objective function  $\varphi$  (as described in section 2.2.1)

and finding the best solution  $(x_{best})$

Initializing initial pulse frequencies  $(f_i)$ , pulse rate  $(r_i)$ , loudness  $(A_i)$

and a set of random numbers  $(rn \in [-1,1])$  with normal distribution

**while** (number of iteration  $(i)$  < maximum number of iteration or stopping criteria met)

Update velocity of bat using  $v_i^t = v_i^{t-1} + (x_i^{t-1} - x_{best})f_i$

where,  $f_i = f_{min} + (f_{max} - f_{min})\beta$ ;  $(\beta \in [0,1])$

Update location of bat using  $x_i^t = x_i^{t-1} + v_i^t$

**if**  $(r_i < rand(0,1))$

Generate a local solution around the existing solution using

$x_i^t(new) = x_i^t(old) + \varepsilon \bar{A}_t$  where,  $(\varepsilon \in rand[-1,1])$  and  $\bar{A}_t$  is the mean of all  $A$  at iteration  $t$

**end if**

Generate a new solution by random flying

**if**  $(rn_1 < A_i \text{ and } fit(x_i^t) < fit(x_{best}^t))$

Accept new solution

Increase pulse rate of the bat using  $r_i^{t+1} = r_i^t(1 - \exp(-\gamma t))$  where,  $\gamma > 0$  is a constant value that controls the movement of bat

Decrease loudness using

$A_i^{t+1} = \alpha A_i^t$  where  $\alpha > 0$  is a constant value controls the movement of bat

**end if**

Find the new best location of the bat  $(x_{best}^{t+1})$

**end while**

### List of abbreviations

<b>2DHE</b>	Two-dimensional histogram equalization
<b>ABC</b>	Artificial bee colony optimization
<b>ACO</b>	Ant colony optimization
<b>AGC</b>	Adaptive gamma correction
<b>AGCWD</b>	Adaptive gamma correction weighted distribution
<b>AGCWHD</b>	Adaptive gamma correction with weighted histogram distribution
<b>AHE</b>	Adaptive histogram equalization
<b>AMSR</b>	Adaptive multi scale Retinex
<b>BA</b>	Bat algorithm
<b>BBHE</b>	Brightness preserving bi-histogram equalization
<b>CEF</b>	contrast enhancement factor
<b>CEFPBHE</b>	Contrast enhancement using feature preservation bi-histogram equalization
<b>CLAHE</b>	Contrast limited adaptive histogram equalization
<b>CLAHE-DGC</b>	Contrast-limited adaptive histogram equalization with dual gamma correction
<b>CSIQ</b>	Categorical image quality database
<b>DCE</b>	Difference channel estimation
<b>DCP</b>	Dark channel priory
<b>DCT</b>	Discrete cosine transform
<b>DCTCH</b>	Discrete cosine transform coefficient histogram
<b>DCTCS</b>	Discrete cosine transform coefficient scaling
<b>DCT-SVD</b>	Discrete cosine transform pyramid and singular value decomposition
<b>DFHE</b>	Dynamic fuzzy histogram equalization
<b>DHE</b>	Dynamic histogram equalization
<b>DSIHE</b>	Dualistic sub-image histogram equalization
<b>FDAHE-GC</b>	Fuzzy dissimilarity adaptive histogram equalization with gamma correction
<b>FDH</b>	Fuzzy dissimilarity histogram
<b>GHE</b>	Global histogram equalization
<b>HSV</b>	Hue, saturation, value
<b>MMBEBHE</b>	Minimum mean brightness error bi-histogram equalization
<b>MSR</b>	Multi scale Retinex
<b>NIQE</b>	Natural image quality evaluator
<b>PCQI</b>	Patch-based contrast quality index
<b>PSO</b>	Particle swarm optimization
<b>RESECDCT</b>	Residual spatial entropy based contrast enhancement using discrete cosine transform
<b>RMMGHT</b>	Recursive median and mean partitioned one-to-one grey level mapping transformations for image enhancement
<b>SECDCT</b>	Spatial entropy-based contrast enhancement in discrete cosine transform
<b>SSR</b>	Single scale Retinex
<b>VBBPDHE</b>	Variance-based brightness preserved dynamic histogram equalization for image contrast enhancement

